Int J Physiol Pathophysiol Pharmacol 2015;7(3):115-125
www.ijppp.org /ISSN:1944-8171/IJPPP0013531

Original Article

The PI3Kδ inhibitor idelalisib suppresses liver and lung cellular respiration

Suleiman Al Hammadi[1], Saeeda Almarzooqi[2], Hidaya Mohammed Abdul-Kader[3], Dhanya Saraswathiamma[2], Abdul-Kader Souid[1]

Departments of [1]Pediatrics, [2]Pathology, [3]Medicine, UAE University, Al-Ain, Abu Dhabi, United Arab Emirates

Received July 27, 2015; Accepted September 9 2015; Epub December 13, 2015; Published December 15, 2015

Abstract: Idelalisib (an inhibitor of phosphatidylinositol-3-kinase-delta) is approved for treatment of B-cell malignancies, with a Boxed Warning concerning potentially fatal hepatic, lung, and intestinal toxicities. The mechanisms of these tissue-specific adverse events have yet to be elucidated. This *in vitro* study investigated whether these effects could be attributed, at least in part, to altered cellular bioenergetics. A phosphorescence analyzer was used to measure cellular mitochondrial O_2 consumption (k_c, μM O_2 min^{-1} mg^{-1}) in C57BL/6 mouse organs in the presence of 10 μM idelalisib or dimethyl-sulfoxide. Idelalisib significantly reduced the rate of cellular respiration in liver and lung fragments by 20% and 27%, respectively. Respiration in intestinal, thymic, and kidney fragments was unaffected. Idelalisib did not alter respiratory chain activities in mitochondria isolated from the liver and did not induce hepatocyte death. Thus, the drug mildly lowers liver and lung cellular respiration, an effect that may contribute to toxicities observed in these organs.

Keywords: Cellular bioenergetics, cellular respiration, idelalisib, liver toxicity, lung toxicity, mitochondrial function, oxidative phosphorylation, PI3K delta, PI3K inhibitors

Introduction

Idelalisib (CAL-101) is the first-in-class inhibitor of phosphatidylinositol-3-kinase delta (PI3Kδ) [1]. This isoform is highly expressed in hematopoietic cells and its inhibition halts B cell viability and proliferation [2, 3]. The enzyme is formed of two subunits, p85 and p110δ; the latter component is selectively blocked (half-maximal effective concentration, 8 nM) by the small molecule inhibitor idelalisib [4, 5].

The U.S. Food and Drug Administration has recently approved the oral idelalisib formulation for treatment (as a single agent or in combination with rituximab) of relapsed chronic lymphocytic leukemia, follicular lymphoma, and small lymphocytic lymphoma. The drug, however, has a Boxed Warning regarding serious hepatotoxicity, diarrhea, colitis, intestinal perforation, and pneumonitis. Other adverse events include myelosuppression and dermatitis [6]. The mechanisms of these potentially fatal and tissue-specific adverse events have yet to be elucidated.

The dual PI3K/mTOR inhibitors GSK2126458, BEZ235, and GDC0980 and the pure mTOR inhibitor sirolimus have been shown to impair cellular bioenergetics (the metabolic reactions involved in energy biotransformation, including cellular respiration and accompanying ATP synthesis) in several murine tissues (the kidney, liver, and heart) [7, 8]. These results are consistent with the known role of mTOR signaling in normal tissue metabolism, including nutrient transport [9-11]. It is unknown, however, whether pure PI3K inhibitors, such as the PI3Kδ inhibitor idelalisib exhibits similar effects, especially in off-target (non-hematopoietic) tissues.

This study investigated the effects of idelalisib on cellular respiration (the process of delivering nutrients and O_2 to the mitochondria, oxidation of reduced metabolic fuels, passage of electrons to O_2, and synthesis of ATP) in murine liver, lung, intestinal, lymphoid and kidney tissues. Its main purpose was to explore whether the idelalisib-induced organ toxicities could be attributed, at least partially, to altered cellular bioenergetics. The other aim of the study was to

investigate the use cellular respiration as a surrogate biomarker for the adverse events of PI3K inhibitors.

Materials and methods

The methods described here were all carried out in "accordance" with the approved guidelines.

Reagents and solutions

Idelalisib {CAL-101; 5-fluoro-3-phenyl-2-[(S)-1-(9H-purin-6-ylamino)-propyl]-3H-quinazolin-4-one; *m.w.* 415.42} was purchased from MedChem Express, LLC (Princeton, NJ); the drug was dissolved in dimethyl sulfoxide (DMSO) at 2.5 mg/mL and stored at -20°C. Pd(II) complex of *meso*-tetra-(4-sulfonatophenyl)-tetrabenzoporphyrin (Pd phosphor) was purchased from Porphyrin Products (Logan, UT). The pancaspase inhibitor zVAD (*N*-benzyloxycarbonyl-val-ala-asp(O-methyl)-fluoromethylketone; *m.w.* = 467.5) was purchased from Calbiochem (La Jolla, CA). The caspase-3 substrate Ac-DEVD-AMC (*N*-acetyl-asp-glu-val-asp-7-amino-4-methylcoumarin; *m.w.* = 675.64) was purchased from Axxora LLC (San Diego, CA). Recombinant human active caspase-3 [0.2 µg/µL in 50 mM Tris-Cl (pH 8.0), 100 mM NaCl, and 50 mM imidazole] was purchased from BD Pharmingen™ (Becton Dickinson & Company, Franklin Lakes, NJ, USA). Rabbit anti-annexin antibody (#D11G2) was purchased from Cell Signaling Technology (Boston, MA, USA). Rabbit anti-cytochrome c antibody [(H-104): sc-7159] was purchased from Santa Cruz Biotechnology, Inc. (Texas, USA). HPLC-grade methanol, RPMI (Roswell Park Memorial Institute) 1640 medium and remaining reagents were purchased from Sigma-Aldrich (St. Louis, MO).

Pd phosphor (2.5 mg/mL = 2 mM, made in dH_2O), glucose oxidase (GO; 10 mg/mL, made in phosphate-buffered saline), Na cyanide (CN, 1.0 M made in dH_2O; pH adjusted to ~7.0 with 12 N HCl), 0.1 M glutamate-malate (made in dH_2O), 0.1 M ADP (made in dH_2O), zVAD (2.14 mM, made in DMSO), and Ac-DEVD-AMC (7.4 mM, made in DMSO) solutions were stored at -20°C.

Mice

C57BL/6 (10 weeks old) mice were housed at 22°C, 60% humidity, and 12-h light-dark cycles. They had *ad libitum* access to standard rodent chow and filtered water. The study was approved from the Animal Ethics Committee-College of Medicine and Health Sciences (A29-13; *In vitro* assessment of the effects of nephrotoxic drugs and toxins on renal cellular respiration in mice).

Tissue collection and processing

Urethane (25% w/v, 100 µL per 10 g) was administered intraperitoneally for anesthesia. A tissue fragment (20 to 40 mg) was then quickly cut from the organ (while it was still well perfused) with a sterile scalpel (Swann-Morton, Sheffield, England). The sample was immersed in ice-cold RPMI saturated with 95% O_2: 5% CO_2, rinsed thoroughly, weighted in the same solution, and immediately placed in the oxygen (glass) vial for measuring cellular respiration at 37°C as described below [16, 17]. The vial contained 1.0 mL RPMI, 3 µM Pd phosphor, 0.5% fat-free albumin, and 10 µM idelalisib (treated condition) or 1.6 µL dimethyl sulfoxide (control condition).

Cellular respiration

Phosphorescence oxygen analyzer was used to monitor cellular mitochondrial O_2 consumption in the tissue fragments as previously described [18, 19]. This analytical method is based on the principle that O_2 quenches phosphorescence. The Pd phosphor Pd(II) complex of *meso*-tetra-(4-sulfonatophenyl)-tetrabenzoporphyrin was used for this purpose [20]. This O_2 probe has an absorption maximum at 625 nm and a phosphorescence maximum at 800 nm. Samples in the measuring chamber were flashed from a pulsed (10 pulses per sec) light-emitting diode array with a peak output at 625 nm (OTL630A-5-10-66-E, Opto Technology, Inc., Wheeling, IL). Emitted phosphoresce was passed through an interference filter centered at 800 nm and detected by a Hamamatsu photomultiplier tube #928. Amplified phosphorescence decay was digitized at 1.0 MHz by a 20-MHz A/D converter using an analog/digital converter PCI-DAS 4020/12 I/O Board (PCI-DAS 4020/12 I/O Board; Computer Boards, Inc., Mansfield, MA).

A software program was developed utilizing the Microsoft Visual Basic 6 programming language, Microsoft Access Database 2007 (Access) database management system, and Universal Library components from the electronic board (http://www.mccdaq.com/daq-

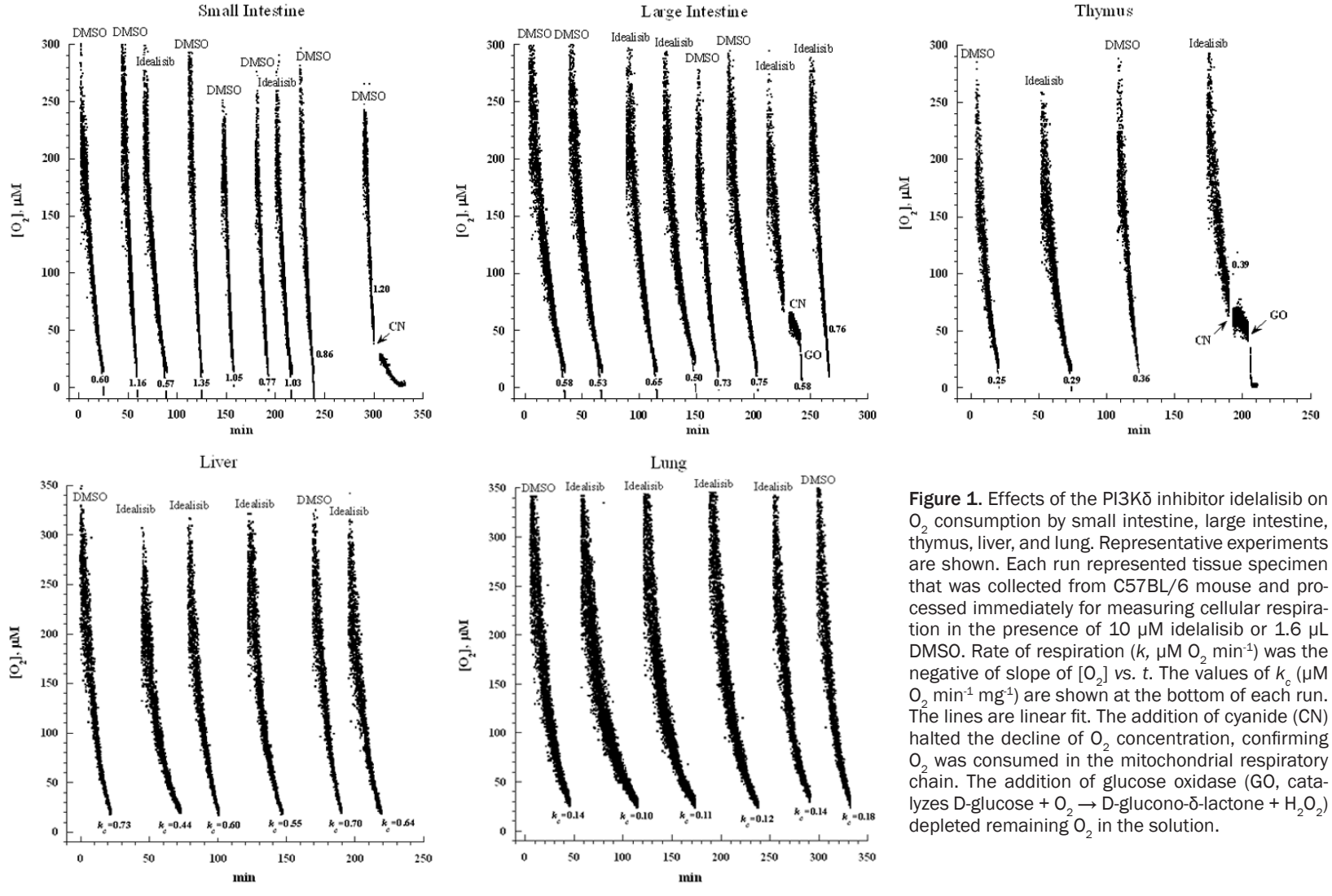

Figure 1. Effects of the PI3Kδ inhibitor idelalisib on O_2 consumption by small intestine, large intestine, thymus, liver, and lung. Representative experiments are shown. Each run represented tissue specimen that was collected from C57BL/6 mouse and processed immediately for measuring cellular respiration in the presence of 10 μM idelalisib or 1.6 μL DMSO. Rate of respiration (*k*, μM O_2 min^{-1}) was the negative of slope of [O_2] *vs*. *t*. The values of k_c (μM O_2 min^{-1} mg^{-1}) are shown at the bottom of each run. The lines are linear fit. The addition of cyanide (CN) halted the decline of O_2 concentration, confirming O_2 was consumed in the mitochondrial respiratory chain. The addition of glucose oxidase (GO, catalyzes D-glucose + O_2 → D-glucono-δ-lactone + H_2O_2) depleted remaining O_2 in the solution.

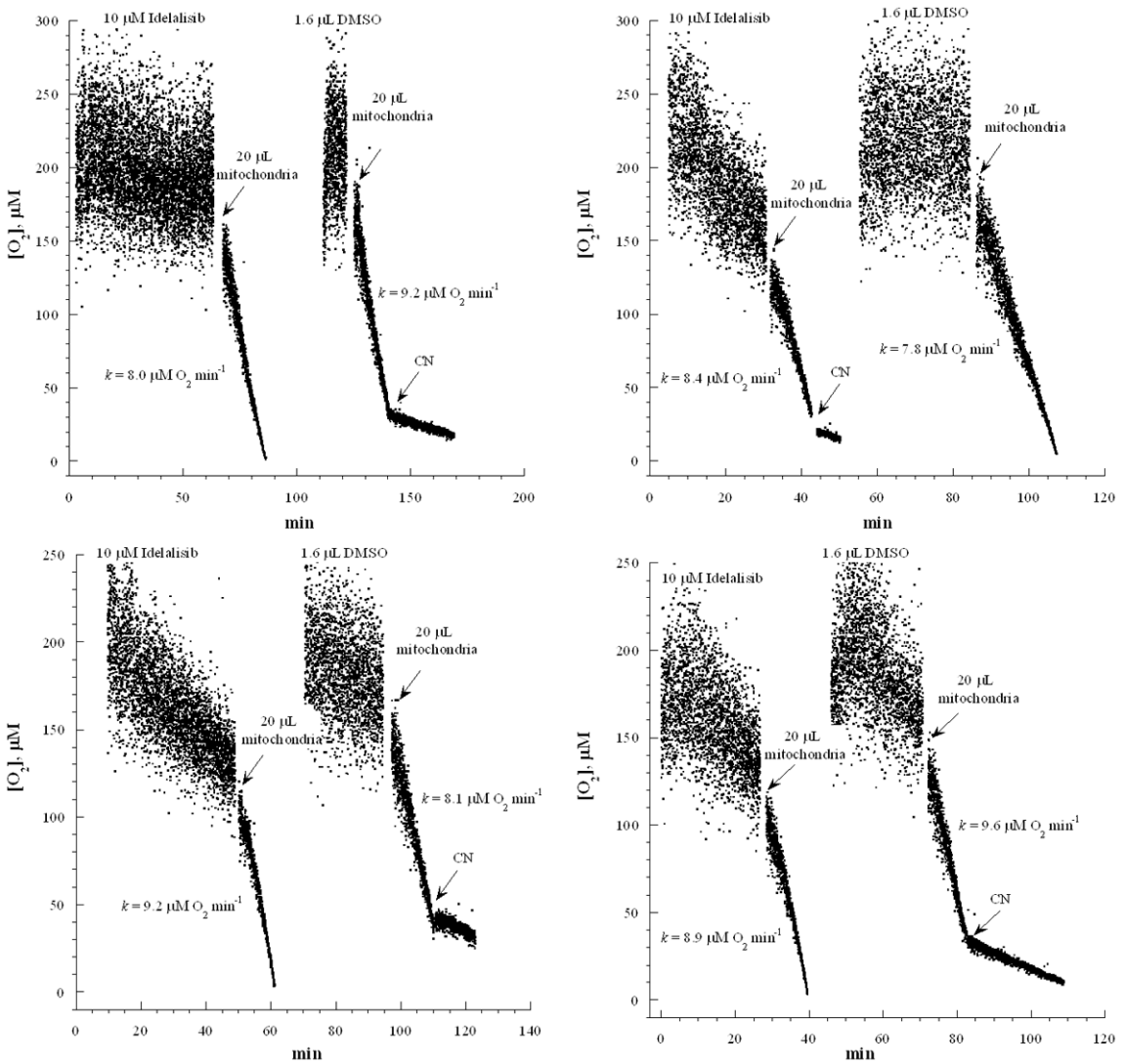

Figure 2. Effects of idelalisib on respiration of isolated mitochondria from mouse liver. Results of four separate experiments are shown. The reaction contained 1.0 mL of 0.1 M Tris/MOPS (pH 7.4), 3 μM Pd phosphor, 1.0 mM glutamate/malate, 1.0 mM ADP, 0.5% fat-free albumin, 20 μL mitochondrial suspension, and 10 μM idelalisib (treated condition) or 1.6 μL DMSO (control condition). Cyanide (CN) inhibited respiration, confirming O_2 was consumed in the respiratory chain. Rate of respiration (*k,* μM O_2 min^{-1}) was the negative of the slope of [O_2] *vs. t*. The values of *k* are shown.

software/universal-library.aspx). The program permitted direct analysis of inputs from the PCI-DAS 4020/12 I/O Board. A relational database was developed to store pulse metadata and slopes. The pulse was identified by detecting 10 phosphorescence intensities above a default voltage. Pulse peak was identified by detecting the highest phosphorescence intensities within a pulse and choosing the data point closest to pulse decay [21].

The phosphorescence decay was a single exponential (R^2 > 0.900); the phosphorescence intensity (I) was expressed as: $I = Ae^{-t/\tau}$. O_2 concentration was determined as a function of time from the phosphorescence decay rate ($1/\tau$) of Pd phosphor. The values of $1/\tau$ were linear with dissolved O_2 concentration ($1/\tau = 1/\tau_o + k_q[O_2]$); where $1/\tau_o$ = phosphorescence decay rate in the absence of O_2; k_q = the second-order O_2 quenching rate constant in sec^{-1}·μM^{-1} [20].

System calibration was performed using the glucose/glucose oxidase system as previously described [19, 20]. (Glucose oxidase catalyzes the reaction: D-glucose + O_2 → D-glucono-δ-

Table 1. Effects of the PI3Kδ inhibitor idelalisib on cellular respiration

	Drug Concentration	k_c (μM O_2 min^{-1} mg^{-1})	Inhibition (%)	*P*
Liver	0	0.71 ± 0.19 (21)	-	-
	10 μM	0.57 ± 0.11 (24)	20	0.028
Lung	0	0.15 ± 0.06 (21)	-	-
	10 μM	0.11 ± 0.05 (21)	27	0.016
Small intestine	0	0.88 ± 0.29 (11)	-	-
	10 μM	0.88 ± 0.16 (10)	0	0.973
Large intestine	0	0.82 ± 0.35 (6)	-	-
	10 μM	0.78 ± 0.28 (8)	5	0.755
Thymus	0	0.31 ± 0.15 (6)	-	-
	10 μM	0.34 ± 0.07 (6)	0	0.394
Spleen	0	0.52 ± 0.09 (4)	-	-
	10 μM	0.50 ± 0.11 (8)	4	0.933
Kidney	0	0.63 ± 0.02 (4)	-	-
	10 μM	0.68 ± 0.13 (8)	0	0.570

Tissue fragments were collected from C57BL/6 mice and immediately processed for measuring cellular respiration in RPMI with and without the designated drugs. The values of k_c are mean ± SD (n).

lactone + H_2O_2). The calibration (O_2 consuming) reaction contained phosphate-buffered saline supplemented with 3 μM phosphor, 0.5% fat-free albumin, 50 μg/mL glucose oxidase, and 0 to 500 μM β-glucose. The values of 1/τ were linear for β-glucose concentrations from 0 to 250 μM (R^2 = 0.8515); the value of k_q (101.1 sec^{-1}·μM^{-1}) was set as the negative of the slope of 1/τ *vs.* [β-glucose] plot [20]. The value of 1/τ for air-saturated solution (in the absence of glucose) was 28,330 sec^{-1} (coefficient of variation = 10%) and for O_2-depleted solution (in the presence of 500 μM β-glucose, i.e., $1/\tau_o$) was 2,875 sec^{-1} (coefficient of variation = 1%). Oxygen concentration (in μM) was set as: $[O_2]$ = (1/τ – 2,875) ÷ 101.1 [19].

Cellular respiration was measured at 37°C in 1-mL sealed glass vials. Mixing was performed with the use of a parylene-coated stirring bar. In these air-sealed vials, $[O_2]$ decreased linearly with time, indicating a zero-order kinetics. The rate of respiration (*k*, in μM O_2 min^{-1}) was the negative of the slope $d[O_2]/dt$; it was normalized by the specimen weight and expressed in (k_c) μM O_2 min^{-1} mg^{-1}. For cellular respiration (**Figure 1**), the respiratory substrates were endogenous cellular metabolic fuels and glucose in the RPMI. For mitochondrial respiration (**Figure 2**), the respiratory substrates were endogenous metabolic fuels and glutamate and malate in the mitochondrial suspension. Cyanide inhibited respiration, confirming O_2 was consumed in the mitochondrial respiratory chain. In addition, the mitochondrial uncoupler carbonilcyanide *p*-triflouromethoxyphenylhydrazone (FCCP) increased the rate of cellular respiration [25].

Isolating liver mitochondria

Mitochondria were isolated from C57BL/6 mouse liver as previously described, except the homogenization solution was 0.25 M sucrose [22]. The O_2 consumption reaction (final volume, 1.0 mL) contained 0.1 M Tris/MOPS (pH 7.4), 3 μM Pd phosphor, 0.5% fat-free albumin, 1.0 mM glutamate/malate, 1.0 mM ADP, 20 μL mitochondrial suspension, and 10 μM idelalisib (treated condition) or 1.6 μL DMSO (control condition).

Liver caspase activity

Intra-hepatocyte caspase activity was measured as previously described [17, 23]. Briefly, liver fragments were incubated at 37°C in RPMI containing 37 μM Ac-DEVD-AMC (caspase-3 substrate) with and without 32 μM zVAD (pan-caspase inhibitor) for 60 min. The control reactions were 37 μM Ac-DEVD-AMC and 0.2 μg recombinant human active caspase-3 with and without 32 μM zVAD. Specimens were disrupted by vigorous homogenization and their supernatants were collected by centrifugation (16,300 g for 90 min) through a Microcentrifuge Filter (m.w. limit = 10,000 Dalton, Sigma©). The solutions were diluted 20 fold in RPMI, separated on HPLC, and analyzed for the free fluorogenic AMC moiety. Reversed-phase HPLC system (Shimadzu i-Series, Japan) was used. Ultrasphere IP column (4.6 × 250 mm) was operated at 25°C and a flow rate of 1.0 mL/min. Solvent A was dH_2O and solvent B was HPLC-grade methanol (isocratic at 0.5 mL/min of each solvent). Run time was 30 min and injection volume 5 μL. Excitation wave length was 380 nm and emission wavelength 460 nm.

Histology and immunoperoxidase staining with annexin A2 and cytochrome c

Liver and lung fragments were fixed in 10% neutral formalin, dehydrated in increasing con-

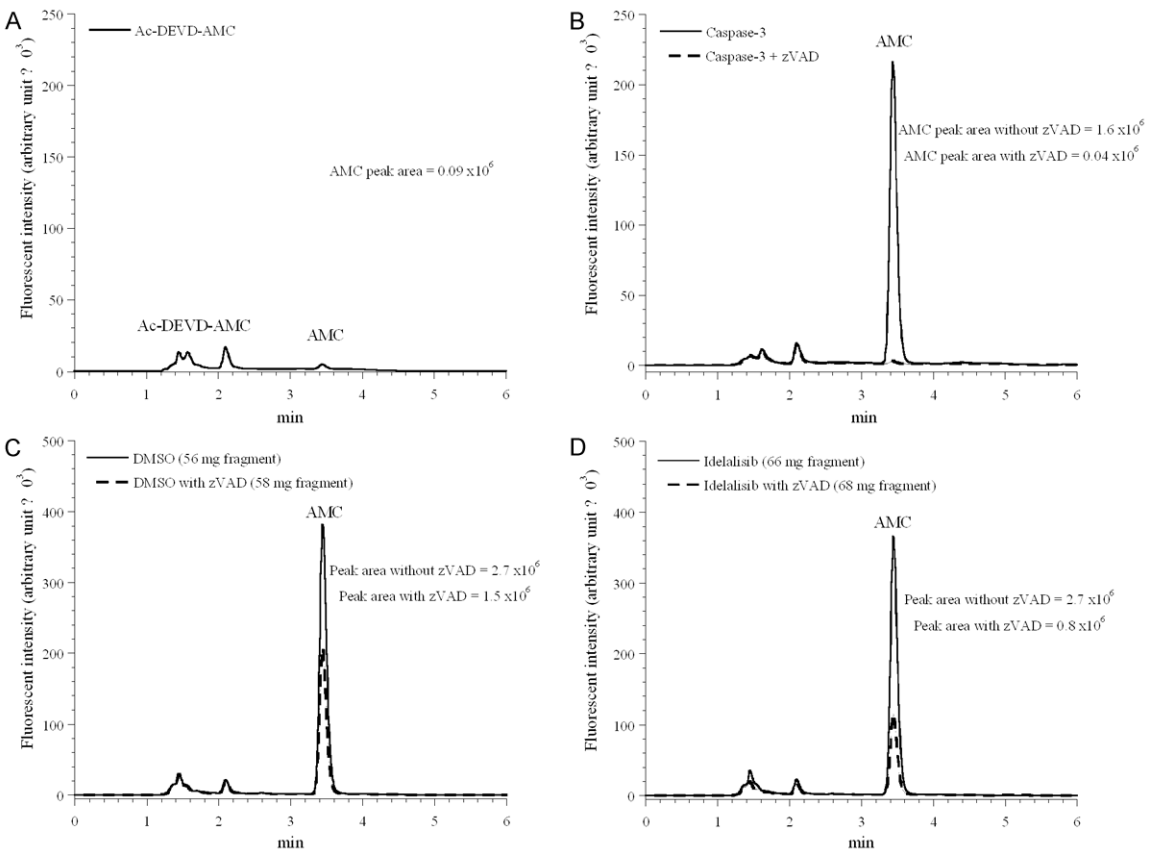

Figure 3. Effects of idelalisib on liver caspase activity. Liver fragments were incubated at 37°C in 25 mL RPMI (intermittently gassed with 95% O_2: 5% CO_2) with 42 µL DMSO or 10 µM idelalisib for 4 h. Specimens were then transferred to the Ac-DEVD-AMC (caspase-3 substrate) cleavage reaction in the presence and absence of zVAD (pancaspase inhibitor) as described in methods. Supernatants of the tissue homogenates were separated on HPLC and analyzed for released AMC moieties (retention time, R_t = 3.44 min). One representative of two separate experiments is shown. (A) Ac-DEVD-AMC alone (R_t = ~1.5 min). (B) Ac-DEVD-AMC plus recombinant human active caspase-3. (C-D) (experiment I): Ac-DEVD-AMC and liver fragments treated with DMSO (C) or idelalisib (D).

centrations of ethanol, cleared with xylene and embedded in paraffin. Tissue sections were prepared from paraffin blocks, stained with hematoxylin and eosin, and immunostained for annexin A2 (1:200 dilution) and cytochrome c (1:500 dilution) as previously described [17]. The immunostaining intensity of annexin A2 was assessed using a manual scoring method: strong (3+), moderate (2+), weak (1+), or negative (0). A score of 0 or 1+ was defined as low annexin A2 immunostaining and a score or 2+ or 3+ was defined as high annexin A2 immunostaining. The percentage of positive cells was also noted [24]. Cytochrome c immunostaining was also assessed as normal pattern of expression (positive in a few bronchiolar, alveolar epithelial cells, and alveolar macrophages) *vs.* abnormal.

Statistical analysis

Data were analyzed on SPSS statistical package (version 19), using the nonparametric (2 independent samples) Mann-Whitney test. *P*-values < 0.05 were considered significant.

Results

Idelalisib reduces the rates of liver and lung cellular respiration

Figure 1 shows representative runs of cellular mitochondrial O_2 consumption by small intestinal, large intestinal, thymic, liver, and lung specimens in the presence and absence of idelalisib. Each run represented a tissue fragment that was collected from the organ, immersed in RPMI, and then immediately placed in the oxy-

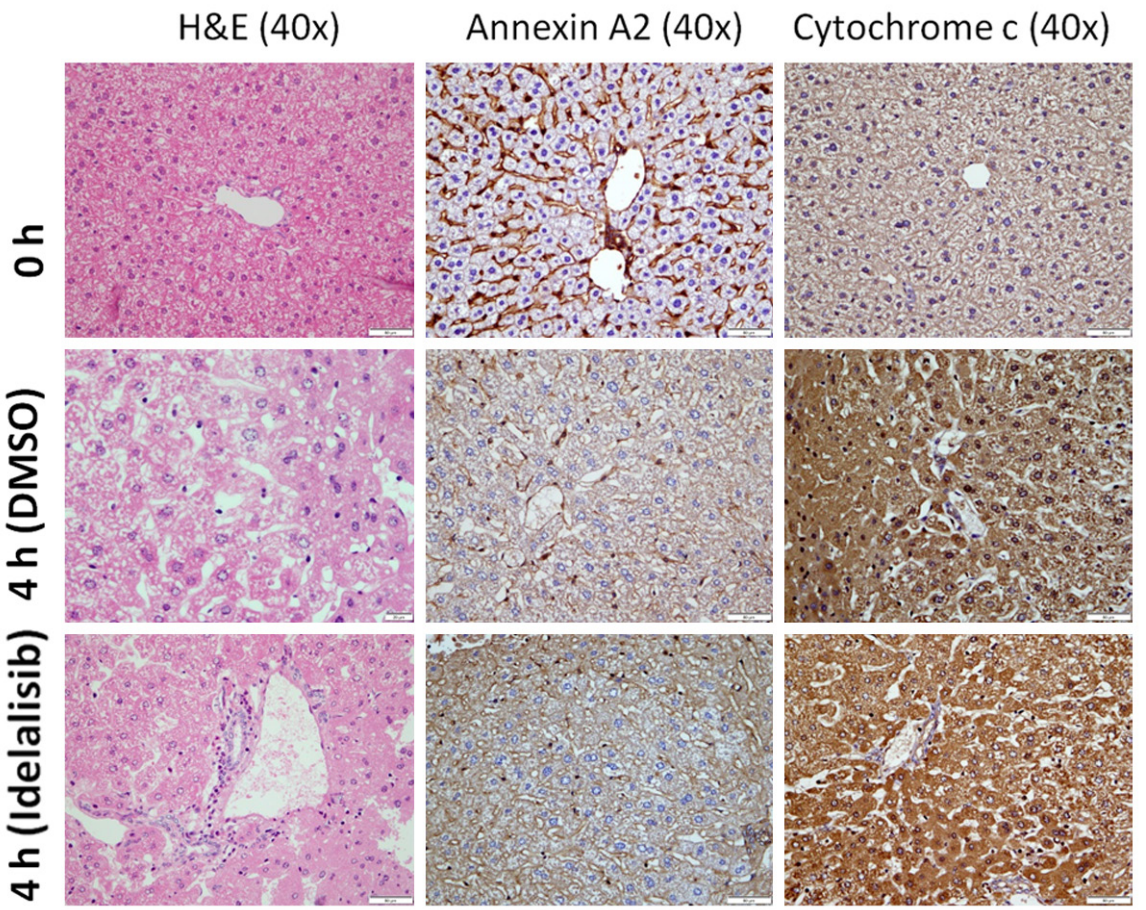

Figure 4. Liver histology and immunoperoxidase staining with annexin A2 and cytochrome c. Liver fragments were incubated at 37°C in 25 mL RPMI (intermittently gassed with 95% O_2: 5% CO_2) with 42 µL DMSO or 10 µM idelalisib for 4 h. Specimens were then stained with H&E and immunostained with annexin A2 and cytochrome c.

gen vial for measuring cellular respiration at 37°C in RPMI with 10 µM idelalisib or 1.6 µL DMSO. The rate of respiration (k_c) was set as the negative of the slope of [O_2] *vs.* *t* plots and expressed in µM O_2 min^{-1} mg^{-1}. The addition of cyanide halted the decline in O_2 concentration, confirming the process occurred in the mitochondrial respiratory chain. The addition of glucose oxidase (catalyzes: D-glucose + O_2 → D-glucono-δ-lactone + H_2O_2) depleted remaining O_2 in the solution.

A summary of all results is shown in **Table 1**. The rate of liver cellular respiration (k_c, mean ± SD) without addition was 0.71 ± 0.19 (n = 21 mice) and with the addition of 10 µM idelalisib was 0.57 ± 0.11 (a 20% decrease, n = 24 mice, P = 0.028). The value of k_c for untreated lung fragments was 0.15 ± 0.06 (n = 21 mice) and for treated lung fragments was 0.11 ± 0.05 (a 27% decrease, n = 21 mice, P = 0.016). In contrast, cellular respiration in the small intestine, large intestine, thymus, spleen, and kidney specimens was unaffected by the idelalisib treatment ($P \geq 0.394$). Thus, idelalisib exhibited a selective suppressive effect on hepatocyte and pneumatocyte respiration. The drugs had no effects on cellular respiration in the other studied organs.

Idelalisib does not directly inhibit mitochondrial respiratory chain complexes

The following experiments were performed to study whether idelalisib acted on the respiratory chain complexes. Mitochondria were isolated from mouse liver and their rates of O_2 consumption (k, µM O_2 min^{-1}) was measured in the presence and absence of 10 µM idelalisib. The respiratory substrates were glutamate and malate. The value of k without idelalisib was 8.7 ± 0.9 and with idelalisib was 8.6 ± 0.5 (n = 4

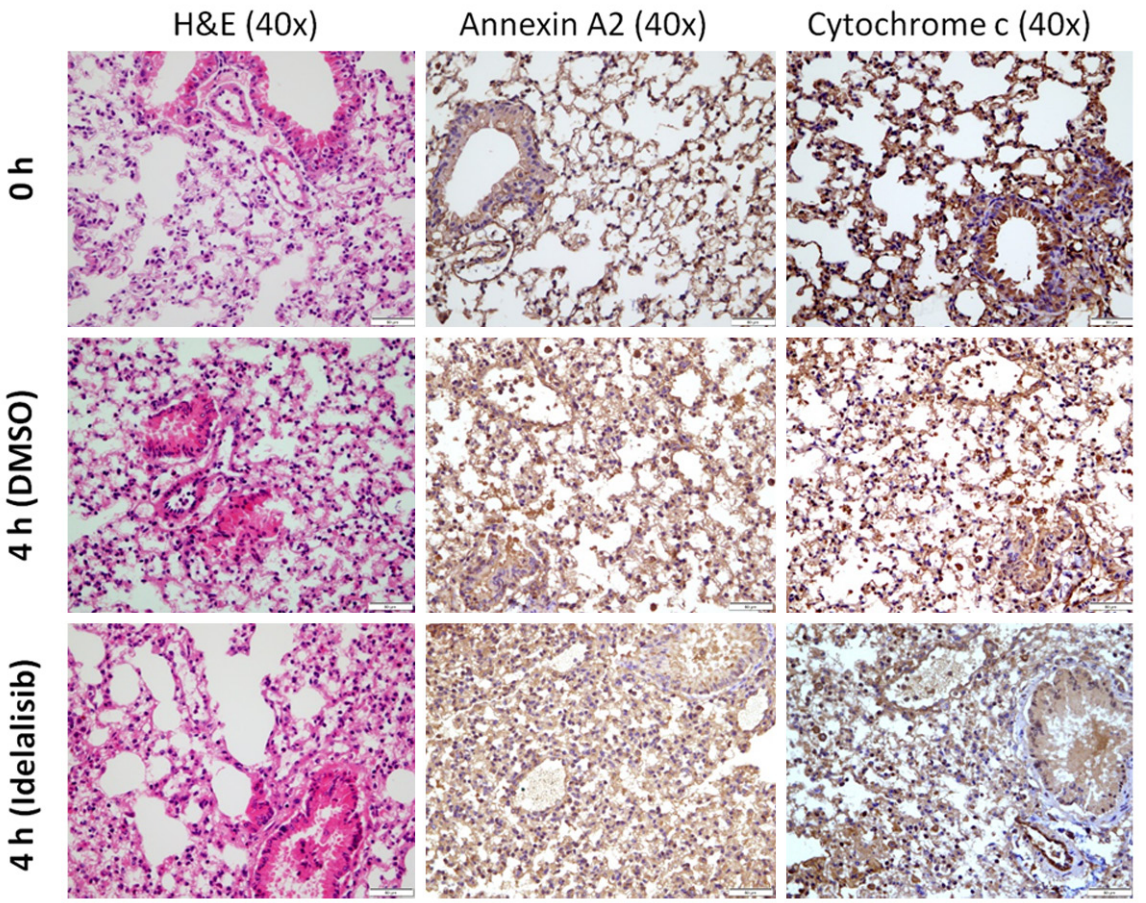

Figure 5. Lung histology and immunoperoxidase staining with annexin A2 and cytochrome c. Lung fragments were incubated at 37 °C in 25 mL RPMI (intermittently gassed with 95% O_2: 5% CO_2) with 42 µL DMSO or 10 µM idelalisib for 4 h. Specimens were then stained with H&E and immunostained with annexin A2 and cytochrome c.

mice, $P = 0.886$), **Figure 2**. Thus, idelalisib did not inhibit metabolic oxidations in the respiratory chain.

Idelalisib treatment does not activate hepatocyte caspases

The following experiments were performed to determine whether idelalisib induces hepatocyte apoptosis. The cleavage of Ac-DEVD-AMC (a caspase-3 substrate analogue) was measured in liver fragments following exposure to DMSO or 10 µM idelalisib for 4 h. The specimen extracts were then separated on HPLC and analyzed for released AMC moieties; one representative of two separate experiments is shown in in **Figure 3C**, **3D**. The AMC peak areas (arbitrary unit $mg^{-1} \div 10^3$) in untreated samples were 49 and 33 and in treated samples were 40 and 42. Thus, idelalisib treatment did not activate hepatocyte caspases. It is worth noting that the AMC area decreased by 58 ± 10% by the pancaspase inhibitor zVAD, confirming cleavage was mediated by caspases (**Figure 3**).

Preserved liver and lung architectures in the presence of idelalisib

The following experiments were performed to study liver and lung histology following exposure to DMSO or 10 µM idelalisib for 4 h. Compared to 0 h, the liver and lung structures were relatively preserved at 4 h in treated and untreated specimens (**Figures 4**, **5**). For both conditions, however, increased hepatocyte vacuolization, single apoptotic cells, and prominent Kupffer cells were noted at 4 h (**Figure 4**). The incubation also resulted in a mild increase in alveolar macrophages (**Figure 5**). Thus, idelalisib treatment did not alter the liver and lung morphology.

Idelalisib treatment does not alter the expression of annexin A2 and cytochrome c

Two apoptotic biomarkers, annexin A2 and cytochrome c were then studied. At 0 h, annexin A2 staining was negative (0) in hepatocytes and positive in sinusoids (internal control). At 4 h, in treated and untreated specimens, annexin A2 staining was positive (3+) in about 5% of hepatocytes, especially those in apoptosis (**Figure 4**). Similarly, at 0 h, cytochrome c staining was negative in hepatocytes. At 4 h, in treated and untreated specimens, cytochrome c staining was positive in hepatocytes, showing moderate expression in background hepatocytes and strong expression in apoptotic cells (**Figure 4**).

At 0 and 4 h (untreated specimen), annexin A2 staining was positive (1+) in alveolar macrophages and a few pneumocytes. At 4 h (treated specimen), annexin A2 staining was mildly increased (2+) in pneumocytes compared to untreated specimen at 4 h (**Figure 5**). Cytochrome c staining was similar in all conditions, showing positivity in a few bronchiolar, alveolar epithelial cells, and alveolar macrophages (**Figure 5**).

Discussion

This study investigated the effects of disrupting PI3Kδ signals on cellular respiration in vital murine organs. Idelalisib significantly lowered liver ($P = 0.028$) and lung ($P = 0.016$) respiration, **Table 1**. These findings may be relevant to the Boxed Warning regarding idelalisib liver and lung toxicities [6]. In contrast, cellular mitochondrial O_2 consumption in five other tissues (thymus, spleen, small intestine, large intestine, and kidney) was unaffected by the idelalisib treatment, $P \geq 0.394$. It is worth noting, however, that the drug exposure was relatively short (about one hour) and the dose was fixed (10 μM). Due to these limitations, it is unknown whether a longer exposure time or a higher dosing would produce changes in these organs.

Methods for isolating mitochondria from murine liver and for measuring intra-hepatocyte caspase activity are well described [17, 22, 23]. These approaches are used here to investigate potential direct effects of idelalisib on the respiration in isolated mitochondria and the intracellular caspase activity. Idelalisib did not alter metabolic oxidations in the respiratory chain of mitochondria isolated from the liver (**Figure 2**). Thus, the mildly decreased cellular respiration observed in the liver and lung is likely related to the known role of mTOR signaling in normal cellular metabolism (e.g., nutrient transport) rather than a direct mitochondrial effect [9-11]. Blocking mTOR prevents glucose uptake, thus, reducing glucose-driven cellular mitochondrial O_2 consumption. In contrast, respiration in isolated mitochondria, driven by the added glutamate/malate, is unaffected by idelalisib. Hepatocyte caspase activity (**Figure 3**), liver and lung architectures (**Figures 4**, **5**), and annexin A2 and cytochrome c expressions (**Figures 4**, **5**) were unaltered in the presence of 10 μM idelalisib for 4 h. Thus, this longer treatment did not induce apoptosis in these organs.

Idelalisib is a highly selective and potent inhibitor of p110δ, with a half-maximal inhibitory concentration against the recombinant enzyme of 8 nM [4, 5]. In one study, the drug exhibited reasonable antitumor activities against hematopoietic malignancies from patients, expressed as percentage EC_{50} (half-maximal effective concentration) relative to 10 μM (the maximum drug concentration used) for each cell type [12]. The same concentration (10 μM) is used here for testing against the studied murine organs (**Table 1**).

In B-cell malignancies, idelalisib also reduced Akt phosphorylation, increased poly(ADP-ribose) polymerase, activated caspases, and induced apoptosis. In murine PDGF (platelet-derived growth factor)-stimulated fibroblasts, 10 μM idelalisib reduced Akt phosphorylation by 25%. By comparison, the drug blocked PI3K signaling in malignant B-cell lines and primary patient tumor cells following cell incubation with 1.0 μM drug for one hour [5].

PI3Kδ has been shown to control intracellular pro-inflammatory cytokines (e.g., trafficking of tumor necrosis factor-α in macrophages) [12]. In one study, blocking PI3Kδ reduced stroke-associated neuroinflammation. The protective mechanism was linked to preventing glucose supply during reperfusion, i.e., blocking the metabolic fuel for aerobic metabolism [13]. These results support a role of PI3Kδ in controlling cellular respiration (aerobic metabolism) in certain organs, including the liver that expresses the delta isoform.

The intestinal toxicity of idelalisib is likely due to B cell depletion, similar to the well-known colitis associated with rituximab treatment [14, 15]. Certainly, the combination of idelalisib and rituximab increases the frequency and severity of this adverse event [6].

It worth noting that the idelalisib-induced B cell death has been linked to the high expression of delta subunit in hematopoietic tissue [2, 3]. Delta subunit activity has been demonstrated in the liver (personal communication with Gilead Sciences); the hepatotoxicity of idelalisib, however, has not been attributed to delta subunit expression in this organ. Similarly, the mechanisms of other tissue-specific toxicities, such as that of the lung have yet to be fully elucidated. The intestinal toxicities, on the other hand, are likely due to B cell depletion, similar to that of rituximab [14, 15]. Intestinal cellular respiration is unaltered by idelalisib (**Figure 1**).

The results here show decreased cellular respiration in organs demonstrating tissue-specific drug toxicities (the liver and lung). Lower cellular respiration implies a defect in any of the following processes: delivering nutrients and O_2 to the mitochondria, oxidation of reduced metabolic fuels, passage of electrons to O_2, and synthesis of ATP. These processes are linked to mTOR signaling in normal tissues [9-11]. As shown in **Figure 2**, idelalisib does not inhibit O_2 consumption in isolated mitochondria. Thus, the drug does not directly interfere with oxidations in the respiratory chain.

In this study, idelalisib was added directly to the tissue rather than dosing the mice. Therefore, more clinically relevant, *in vivo* studies are needed to overcome this potential limitation.

In conclusion, the results show the PI3Kδ inhibitor idelalisib lowers hepatocyte and pneumatocyte respiration. The drug, however, has no effects on cellular respiration in the other studied organs. Idelalisib treatment does not alter respiratory chain activities in isolated mitochondria. The drug does not induce morphologic changes or apoptosis in liver and lung tissues. The results may also support the use of cellular respiration as a surrogate biomarker for the activities and adverse events of PI3K inhibitors [16].

Acknowledgements

This research was funded by Startup Grant and NRF 31M096 grant from the UAE University.

Disclosure of conflict of interest

None.

Address correspondence to: Abdul-Kader Souid, Department of Pediatrics, UAE University, Al-Ain, Abu Dhabi, United Arab Emirates. Tel: +971-3-713-7429; +971-50-723-7850; Fax: +971-3-713-7333; E-mail: asouid@uaeu.ac.ae

References

[1] Gopal AK, Kahl BS, de Vos S, Wagner-Johnston ND, Schuster SJ, Jurczak WJ, Flinn IW, Flowers CR, Martin P, Viardot A, Blum KA, Goy AH, Davies AJ, Zinzani PL, Dreyling M, Johnson D, Miller LL, Holes L, Li D, Dansey RD, Godfrey WR, Salles GA. PI3Kδ inhibition by idelalisib in patients with relapsed indolent lymphoma. N Engl J Med 2014; 370: 1008-1018.

[2] Vanhaesebroeck B, Guillermet-Guibert J, Graupera M, Bilanges B. The emerging mechanisms of isoform-specific PI3K signaling. Nat Rev Mol Cell Biol 2010; 11: 329-341.

[3] Vanhaesebroeck B, Stephens L, Hawkins P. PI3K signalling: the path to discovery and understanding. Nat Rev Mol Cell Biol 2012; 13: 195-203.

[4] Okkenhaug K, Bilancio A, Farjot G, Priddle H, Sancho S, Peskett E, Pearce W, Meek SE, Salpekar A, Waterfield MD, Smith AJ, Vanhaesebroeck B. Impaired B and T cell antigen receptor signaling in p110delta PI 3-kinase mutant mice. Science 2002; 297: 1031-1034.

[5] Lannutti BJ, Meadows SA, Herman SE, Kashishian A, Steiner B, Johnson AJ, Byrd JC, Tyner JW, Loriaux MM, Deininger M, Druker BJ, Puri KD, Ulrich RG, Giese NA. CAL-101, a p110delta selective phosphatidylinositol-3-kinase inhibitor for the treatment of B-cell malignancies, inhibits PI3K signaling and cellular viability. Blood 2011; 117: 591-594.

[6] U.S. Food and Drug Administration Approves Gilead's Zydelig® (idelalisib) for Relapsed Chronic Lymphocytic Leukemia, Follicular Lymphoma and Small Lymphocytic Lymphoma. Available at: http://www.gilead.com/news/press-releases#sthash.4TWDJpRo.dpuf. (Accessed: 12th November 2014).

[7] Almarzooqi S, Albawardi A, Alfazari AS, Saraswathiamma D, Abdul-Kader HM, Shaban S, Mallon R, Souid AK. Effects of selected inhibitors of protein kinases and phosphatases on cellular respiration: an *in vitro* study. J Clin Toxicol 2014; 4: 212.

[8] Albawardi A, Almarzooqi S, Saraswathiamma D, Abdul-Kader HM, Souid AK, Alfazari AS. The mTOR inhibitor sirolimus suppresses renal, hepatic, and cardiac tissue cellular respiration. Int J Physiol Pathophysiol Pharmacol 2015; 7: 54-60.

[9] Schieke SM, Phillips D, McCoy JP Jr, Aponte AM, Shen RF, Balaban RS, Finkel T. The mammalian target of rapamycin (mTOR) pathway regulates mitochondrial oxygen consumption and oxidative capacity. J Biol Chem 2006; 281: 27643-27652.

[10] Cunningham JT, Rodgers JT, Arlow DH, Vazquez F, Mootha VK, Puigserver P. mTOR controls mitochondrial oxidative function through a YY1-PGC-1α transcriptional complex. Nature 2007; 450: 736-740.

[11] Tennant DA, Durán RV, Gottlieb E. Targeting metabolic transformation for cancer therapy. Nat Rev Cancer 2010; 10: 267-277.

[12] Low PC, Misaki R, Schroder K, Stanley AC, Sweet MJ, Teasdale RD, Vanhaesebroeck B, Meunier FA, Taguchi T, Stow JL. Phosphoinositide 3-kinase δ regulates membrane fission of Golgi carriers for selective cytokine secretion. J Cell Biol 2010; 190: 1053-1065.

[13] Low PC, Manzanero S, Mohannak N, Narayana VK, Nguyen TH, Kvaskoff D, Brennan FH, Ruitenberg MJ, Gelderblom M, Magnus T, Kim HA, Broughton BR, Sobey CG, Vanhaesebroeck B, Stow JL, Arumugam TV, Meunier FA. PI3Kδ inhibition reduces TNF secretion and neuroinflammation in a mouse cerebral stroke model. Nat Commun 2014; 5: 3450.

[14] Freeman HJ. Colitis associated with biological agents. World J Gastroenterol 2012; 18: 1871-1874.

[15] El Fassi D, Nielsen CH, Kjeldsen J, Clemmensen O, Hegedüs L. Ulcerative colitis following B lymphocyte depletion with rituximab in a patient with Graves' disease. Gut 2008; 57: 714-715.

[16] Al-Hammadi S, Alfazari AS, Shaban S, Souid AK. Study on the use of cellular respiration as a surrogate biomarker in drug development. Austin J Clin Pathol 2014; 1: 7.

[17] Alfazari AS, Almarzooqi S, Albawardi A, Sami Shaban, Al-Dabbagh B, Saraswathiamma D, Tariq S, Souid AK. *Ex vivo* study on the effects of sorafenib and regorafenib on murine hepatocytes. J Clinl Toxicol 2014; 4: e207.

[18] Souid AK, Tack KA, Galvan KA, Penefsky HS. Immediate effects of anticancer drugs on mitochondrial oxygen consumption. Biochem Pharmacol 2003; 66: 977-987.

[19] Al-Jasmi F, Al Suwaidi AR, Al-Shamsi M, Marzouqi F, Almansouri A, Shaban S, Penefsky HS, Souid AK. Phosphorescence oxygen analyzer as a measuring tool for cellular bioenergetics. In: Clark K, editor. *Biochemistry, Genetics and Molecular Biology*. InTechOpen; 2012; Ch. 10: pp. 237-256.

[20] Lo LW, Koch CJ, Wilson DF. Calibration of oxygen-dependent quenching of the phosphorescence of Pd-meso-tetra (4-carboxyphenyl) porphine: A phosphor with general application for measuring oxygen concentration in biological systems. Anal Biochem 1996; 236: 153-160.

[21] Shaban S, Marzouqi F, Almansouri A, Penefsky HS, Souid AK. Oxygen measurements via phosphorescence. Comput Methods Programs Biomed 2010; 100: 265-268.

[22] Frezza C, Cipolat S, Scorrano L. Organelle isolation: functional mitochondria from mouse liver, muscle and cultured fibroblasts. Nat Protoc 2007; 2: 287-295.

[23] Tao Z, Penefsky HS, Goodisman J, Souid AK. Caspase activation by cytotoxic drugs (the caspase storm). Mol Pharm 2007; 4: 583-595.

[24] Lokman NA, Elder AS, Ween MP, Pyragius CE, Hoffmann P, Oehler MK, Ricciardelli C. Annexin A2 is regulated by ovarian cancer-peritoneal cell interactions and promotes metastasis. Oncotarget 2013; 4: 1199-1211.

[25] Al Samri MT, Al Shamsi M, Al-Salam S, Marzouqi F, Mansouri A, Al-Hammadi S, Balhaj G, Al Dawaar SK, Al Hanjeri RS, Benedict S, Sudhadevi M, Conca W, Penefsky HS, Souid AK. Measurement of oxygen consumption by murine tissues *in vitro*. J Pharmacol Toxicol Methods 2010; 63: 196-204.